IEEE Access
Multidisciplinary | Rapid Review | Open Access Journal

Received August 19, 2019, accepted September 3, 2019, date of publication September 6, 2019,
date of current version September 23, 2019.

Digital Object Identifier 10.1109/ACCESS.2019.2939789

A Novel Scheme for Detection and Estimation of Unresolved Targets With Stepped-Frequency Waveform

SHENGBIN LUO WANG, ZHEN-HAI XU, XINGHUA LIU, WEI DONG, AND GUOYU WANG
State Key Laboratory of Complex Electromagnetic Environment Effects on Electronics and Information System, National University of Defense Technology, Changsha 410005, China

Corresponding author: Zhen-Hai Xu (drxzh930@sina.com)

This work was supported in part by the National Nature Science Foundation of China under Grant 61471372, and in part by the Foundation of National Key Laboratory of Antennas and Microwave Technology under Grant 61424020301162402005.

ABSTRACT The "masking effect" of unresolved targets always results in missed detection and inaccurate parameter estimation. A feasible approach to separate the unresolved targets is improving the range resolution by increasing the signal bandwidth. In this paper, we propose a novel scheme to detect and measure the unresolved targets for the phased array radar with stepped-frequency waveform, which provides a large synthetic bandwidth. We establish the signal model of the stepped-frequency pulse train and review the conventional 1-D High Range Resolution Profile (HRRP). Since the 1-D HRRP of each element fails to integrate the spatial domain, we develop a 2-D HRRP where the target echo can be effectively integrated both in time and spatial domains. Specifically, the 2-D HRRP is generated by the range-angle beamforming technique. In order to address the range shift in the 2-D HRRP caused by target motion, we design a short-long stepped-frequency pulse train as the transmit waveform, which contains a short pulse subtrain with a small pulse repetition interval (PRI) and a long pulse subtrain with a large PRI. The proposed scheme includes two parts of beamforming detection and parameter estimation with range shift elimination. Based on two 2-D HRRPs generated by short and long pulse subtrains, each target can be successfully detected by beamforming detection and target's range, angle and velocity can be accurately estimated by parameter estimation with range shift elimination. Simulation results demonstrate the effectiveness of the proposed scheme.

INDEX TERMS Stepped-frequency waveform, detection and parameter estimation, unresolved targets, high range resolution profile (HRRP), short-long stepped-frequency pulse train.

I. INTRODUCTION

Unresolved targets denote the targets located in the same resolution cell, i.e., the multiple closely-spaced targets which cannot be resolved in time, frequency or spatial domain [1]. The unresolved targets are common in the radar application, such as early warning and low-angle tracking. However, the conventional signal processing, like monopulse processing and Moving Target Detection (MTD), may fail in the case of unresolved targets because their echoes interfere with each other, which is also referred to as "masking effect" [2]. The target number is always underestimated (i.e., missed detection) and the estimated parameters wander far beyond the true values due to such effect [3]. How to achieve detection and parameter estimation of the unresolved targets is still an open issue.

There were many attempts to detect and measure the unresolved targets with monopulse processing. A number of angular resolution methods [4]–[9] were reported over the last two decades. However, such methods are only valid for the two-target case. To break through this limitation, the angle domain is combined with the range domain to obtain more processing degrees of freedom. In [10], a joint range bin processing was proposed to detect and localize the unresolved targets, where at most five targets can be separated in range-angle domain. In [11], [12], the joint range sampling is incorporated into a statistical model for the target with pulse-to-pulse fluctuation to achieve target localization. However, only the rectangular pulse is taken into account as the transmit waveform.

The associate editor coordinating the review of this manuscript and approving it for publication was Weimin Huang.

That is, the joint range bin processing is unavailable when transmitting the complex waveform, e.g. Linear Frequency Modulation (LFM) pulse. Meanwhile, the parameter estimation is achieved by the method of moment. A high Signal-to-Noise Ratio (SNR) or a long span of observation time are required, which is often limited in practice especially in the long-range detection and tracking. Moreover, the performance will get worse without accurately modeling the targets.

Most of the existing work try to resolve multiple targets in the same resolution cell based on statistical model or parametric model. However, the most effective approach is improving the radar resolution. It is much difficult to improve the radar resolutions of angle and velocity because they are determined by the antenna aperture and the observation time, which are fundamentally limited by the system cost and the time resource referred to dwell scheduling. In contrary, the range resolution can be easily improved by synthesizing the diverse frequencies of multiple pulses to generate the High Range Resolution Profile (HRRP). That is, the range resolution ability can be improved by the transmit waveform design in time domain. In the HRRP, the unresolved targets can be resolved in range domain as long as the synthetic bandwidth is large enough.

One of the common approaches to generating HRRP is the stepped-frequency waveform technique. A definite advantage of using stepped-frequency waveform is the low system cost because only a narrow instantaneous receiver bandwidth is required. However, such waveform is much sensitive to target motion, which is the so-called "Doppler effect" [13], especially when considering a target with a large radial velocity. The Doppler effect causes additional linear phase term and quadratic phase term, which induces the distortion of HRRP. Specifically, the linear phase term results in the range shift of peak position, and the quadratic phase term results in the spread of peak shape [14]. Due to the distortion of HRRP, the detection and estimation performance of unresolved targets degrades greatly. Thus, motion compensation is the key issue for the application of HRRP.

A large number of methods are proposed for the motion compensation. One approach is the velocity compensation, where target's velocity is estimated precisely to compensate the phase error caused by target motion. A velocity estimator based on Maximum Likelihood (ML) principle is developed in [15]. To improve the estimation accuracy, the nonlinear least squares principle is used in [16]. However, such approach is not available in the case of unresolved targets because the masking effect will cause a severe estimation error. In [17], the Minimum Description Length (MDL) principle is combined with ML principle to resolve multiple targets. However, a large computational cost is required for a good performance. The other approach is waveform design, where the waveform is designed specially to eliminate the range shift. In [18]–[20], the pulse train is divided into multiple pulse subtrains with different stepped frequencies. The HRRP of each substrain has different range shift and the true value of target position can be solved. To reduce the sidelobe of HRRP, the phase coding is also used in waveform design, including polyphase coding [21], [22] and Costas coding [23]. However, such methods are invalid in multitarget. Moreover, most of the motion compensation methods are not available on the phased array radar since target's angle and range are coupled in the phase term.

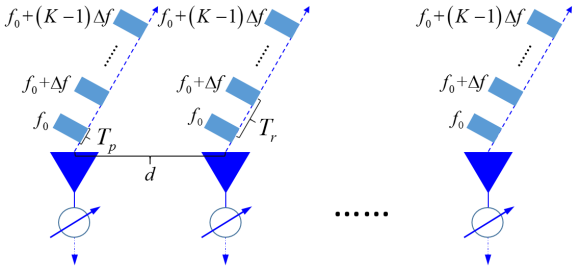

FIGURE 1. Illustration of stepped-frequency pulse train transmitted by phased array radar.

It is feasible to separate the unresolved targets in range domain by using the stepped-frequency waveform. In this paper, based on the stepped-frequency waveform, we propose a novel scheme to detect and measure the unresolved targets for the phased array radar. Specifically, we spacially design the transmit waveform for motion compenation. In the sequel, the corresponding method is developed to achieve the detection and parameter estimation of unresolved targets. Our contributions are summarized as follows: 1) Beamforming detection. The range-angle beamforming technique is used to generate the 2-D HRRP in range-angle domain, where target acho can be effectively integrated both in time and spatial domains. Then we develop the beamforming detection based on the Constant False Alarm Rate (CFAR) technique. Each target can be detected successfully with the beamforming detection. 2) Parameter estimation with range shift elimination. We specially design a short-long stepped-frequency pulse train as the transmit waveform, which contains two pulse subtrains with different Pulse Repetition Interval (PRI). By combining the 2-D HRRPs generated by two pulse subtains, the range shift can be eliminated and each target's range, angle and velocity can be estimated accurately.

The rest of paper is organized as follows. We firstly give the signal model of stepped-frequency waveform for the phased array radar in Section II. Next, we present the scheme to detect and measure the unresolved targets in Section III. Then several simulation results are shown in Section IV. Finally, the conclusions are drawn in Section V.

II. PROBLEM FORMULATION

A. SIGNAL MODEL

Consider a uniform linear array with N elements whose interval is d. To achieve high range resolution, a stepped-frequency LFM pulse train is used as the transmit waveform. As shown in Fig. 1, K pulses are transmitted in repetition T_r. Bandwidth and duration of each pulse are B_p and T_p respectively, and the carrier frequency is stepped from pulse

to pulse. The transmit signal is then expressed as

$$s(t) = \sum_{k=0}^{K-1} p(t - kT_r)e^{j2\pi f_k t} \tag{1}$$

where $p(t) = \text{rect}[(t - T_p/2)/T_p]e^{j\pi\mu t^2}$ is the waveform of LFM pulse and $f_k = f_0 + k\Delta f$ $(k = 0, 1, \cdots, K-1)$ is the carrier frequency. $\mu = B_p/T_p$ denotes the frequency modulation rate.

Firstly, we focus on the case of one single target in uniform motion whose range, angle and radial velocity are R, θ and v. Taking the first element as reference, the target echo received by the nth $(n = 0, 1, \cdots, N-1)$ element is

$$r_n(t) = \alpha e^{-j\frac{2\pi}{c}f_k ndu} \cdot s(t - \frac{2R}{c} + \frac{2vt}{c}) \tag{2}$$

where α is the complex reflection coefficient and $u = \sin\theta$ is the angle cosine. We take $s_0 = p(t)e^{j2\pi f_k t}$ as the reference signal of matching filter. In the sequel, the filtered signal is expressed as

$$Z_n(t) = \alpha e^{-j\frac{2\pi}{c}f_k ndu} \int_{-\infty}^{\infty} s(\tau - \frac{2R}{c} + \frac{2vt}{c})s_0^*(\tau - t)d\tau \tag{3}$$

where $[\cdot]^*$ denotes the conjugate operator. After reasonable approximation and demodulation processing (See Appendix A), we give the baseband signal of the nth element as

$$Z_n'(t) = \alpha' \sum_{k=0}^{K-1} \left|\chi(t - \frac{2R}{c} - kT_r, \frac{2v}{c}f_k)\right| \cdot e^{-jn\Theta u}e^{-jk(\Phi R - \Psi v + n\xi\Theta u)}e^{-jk^2\xi\Psi v} \tag{4}$$

where $\alpha' = \alpha e^{-j\frac{4\pi}{c}f_0 R + \phi(t)}$, $\Theta = 2\pi f_0 d/c$, $\Phi = 4\pi\Delta f/c$, $\Psi = 4\pi T_r f_0/c$, $\xi = f_0/\Delta f$. $\phi(t)$ is the phase of $\chi(t - 2R/c - kT_r, f_k 2v/c)$ and $\chi(t, f_d)$ denotes the ambiguity function of LFM pulse expressed as

$$\chi(t, f_d) = \int_{-\infty}^{\infty} p(\tau)p^*(\tau - t)e^{j2\pi f_d \tau}\mathrm{d}\tau \tag{5}$$

Note that, K peaks appear in the baseband signal at time $t = 2R/c + kT_r$. Assume that there is no target migration through resolution cell and the maximum values are located at $t_s(k+1) = l\Delta t + kT_r$ where Δt is the sampling time interval. We pick up the peaks of sampled baseband signal to generate a $K \times N$ data matrix expressed as

$$\begin{aligned}\boldsymbol{X} &= \begin{bmatrix} Z_0'[t_s(1)] & Z_0'[t_s(2)] & \cdots & Z_0'[t_s(K)] \\ Z_1'[t_s(1)] & Z_1'[t_s(2)] & & Z_1'[t_s(K)] \\ \vdots & \vdots & \cdots & \vdots \\ Z_{N-1}'[t_s(1)] & Z_{N-1}'[t_s(2)] & & Z_{N-1}'[t_s(K)] \end{bmatrix} \\ &= \begin{bmatrix} \boldsymbol{x}_0^T & \boldsymbol{x}_1^T & \cdots & \boldsymbol{x}_{N-1}^T \end{bmatrix}^T \\ &= \boldsymbol{A}\boldsymbol{S}(R, u, v) + \boldsymbol{N} \end{aligned} \tag{6}$$

where $[\cdot]^T$ denotes the transport operation, $\boldsymbol{S}(R, u, v)$ and $\boldsymbol{N}$ denote the steering matrix and the noise matrix respectively. $\boldsymbol{A}$ is a diagnose matrix expressed as

$$\boldsymbol{A} = \begin{bmatrix} A_0 & 0 & \cdots & 0 \\ 0 & A_1 & \cdots & 0 \\ \vdots & \vdots & \ddots & \vdots \\ 0 & 0 & \cdots & A_{K-1} \end{bmatrix} \tag{7}$$

where $A_k = \alpha'|\chi(l\Delta t - 2R/c, 2vf_k/c)|$ denotes the complex amplitude of the kth filtered pulse. Element of the nth row and the kth column in $\boldsymbol{S}$ is

$$S_{n,k}(R, u, v) = e^{-jn\Theta u}e^{-jk(\Phi R - \Psi v + n\xi\Theta u)}e^{jk^2\xi\Psi v} \tag{8}$$

It should be noted that the Doppler frequency turns to higher with the increasing carrier frequency, which results in the degressive output amplitude of matching filter. That is, $|A_0| > |A_1| > \cdots > |A_{K-1}|$. It is aimed to separate the unresolved targets by improving the range resolution. The high range resolution is exactly close to target size. In this sense, the difference between amplitudes is negligible because Δf we needed is not large. Therefore, we have $A_0 \approx A_1 \approx \cdots \approx A_{K-1} = A$ and $\boldsymbol{A} = A\boldsymbol{I}$, where $\boldsymbol{I}$ is a unit matrix. In the sequel, (6) is rewritten as

$$\boldsymbol{X} = A\boldsymbol{S}(R, u, v) + \boldsymbol{N} \tag{9}$$

Then, we consider the case of unresolved targets. Assume that there are M targets in the same resolution cell (R_0, u_0, v_0). In this case, the signal model is rewritten as

$$\boldsymbol{X} = \sum_{m=1}^{M} A_m \boldsymbol{S}(R_m, u_m, v_m) + \boldsymbol{N} \tag{10}$$

where A_m and (R_m, u_m, v_m) are the mth target's complex amplitude and parameters needed to be estimated. Since all targets are not resolved in each domain, we then have $|R_m - R_0| < \Delta R/2$, $|u_m - u_0| < \Delta u/2$ and $|v_m - v_0| < \Delta v/2$, where ΔR, Δu and Δv are the radar resolutions in range, angle and velocity. They are expressed as

$$\begin{aligned} \Delta R &= c/2B_p \\ \Delta u &= c/f_0 Nd \\ \Delta v &= c/2f_0 KT_r \end{aligned} \tag{11}$$

In particular, ΔR we defined here is a coarse range resolution for a single LFM pulse with small bandwidth, but not for the synthetic bandwidth of stepped-frequency pulse train. We define the element-based SNR of each target as $\text{SNR}_m = |A_m|^2/\sigma^2$ where σ^2 denotes the noise power.

B. 1-D HRRP OF UNRESOLVED TARGETS

We aim to detect each target and estimate each target's parameters. That is to determine M and (R_m, u_m, v_m). However, M is usually underestimated in the case of unresolved targets. Moreover, the conventional methods of parameter measurement, such as monopulse technique and MTD, are invalid. In theory, we can improve the range resolution by transmitting the stepped-frequency pulse train and use the 1-D HRRP

to resolve multiple targets in range domain. Usually, the 1-D HRRP is generated by Inverse Discrete Fourier Transform (IDFT). The IDFT processing of stepped-frequency pulse train is equivalent to the beamforming in range domain indeed. 1-D HRRP of the nth element is

$$\begin{aligned} O_n(R) &= \boldsymbol{w}^H(R)\boldsymbol{x}_n^T \\ &= \sum_{m=1}^{M} A_m e^{-jn\Theta u_m} \\ &\quad \cdot \sum_{k=0}^{K-1} e^{jk^2\xi\Psi v_m} e^{-jk[\Phi(R_m-R)-\Psi v_m+n\xi\Theta u_m]} \end{aligned} \tag{12}$$

where $\boldsymbol{w}^H(R) = \left[1 \; e^{-j\Phi R} \cdots e^{-j(K-1)\Phi R}\right]^T$ is the wight of range beamforming and $[\cdot]^H$ is the conjugate transpose operator.

In (12), there are a 1st order phase component $k[\Phi(R_m - R) - \Psi v_m + n\xi\Theta u_m]$ and a 2nd order phase component $k^2\xi\Psi v_m$. The 1st order phase component determines the peak position of 1-D HRRP, and the 2nd order phase component results in the power spread but not affect the peak position [14]. The peaks of HRRP appear at [18]

$$R = R_m - \Psi v_m/\Phi + n\xi\Theta u_m/\Phi \tag{13}$$

From (12), we can see that the beamformer output is the sum of multiple targets' 1-D HRRPs, which results in inaccurate ranging and missed detection. From (13), it is observed that the peak have a shift from the true value. Such range shift is not only caused by target's velocity, but also by target's angle, which causes that the peak position of 1-D HRRP has a migration during elements. That is, 1-D HRRP of each element cannot be integrated effectively in spatial domain, which fundamentally limits the performance of target detection. The conventional processing of stepped-frequency waveform, only focusing on target motion compensation, is not available here. Such range shift can be eliminated if target's angle and velocity are estimated. However, as mentioned above, the conventional methods cannot provide an accurate parameter estimation in the case of unresolved targets. Therefore, 1-D HRRP is not suitable for the phased array radar to detect and measure the unresolved targets.

III. SCHEME FOR DETECTION AND PARAMETER ESTIMATION OF UNRESOLVED TARGETS

In this section, a novel scheme for detection and parameter estimation of the unresolved targets is proposed. We design a short-long stepped-frequency pulse train and develop the corresponding methods to detect and measure the unresolved targets. The scheme includes two parts of beamforming detection and parameter estimation with range shift elimination. By the proposed scheme, each target can be detected successfully and target's parameters (i.e., range angle and velocity) can be estimated accurately.

A. RANGE-ANGLE BEAMFORMING AND 2-D HRRP

The stepped-frequency waveform has been developed to improve the HRRP for a single-antenna radar. However, regarding the antenna array radar, the 1-D HRRP fails in the integration of spatial domain because target's range, angle and velocity are all coupled in the phase term. Even though the stepped-frequency waveform provides a large synthetic bandwidth, the range resolution ability is still poor without effective energy integration. To break through the limination of 1-D HRRP, we use the range-angle beamforming technique [24] here. The beamformer can generate a 2-D HRRP in range-angle domain, which provides a promising resolution ability in range-angle domain to separate the unresolved targets.

The range-angle beamforming is a development of digital beamforming technique where a digital receive beam is steered to search a specific area in range-angle domain by using two-dimensional weighting. In the case of unresolved targets, we only need to consider the beamformer output in the resolution cell (R_0, u_0, v_0) where multiple targets found. The two-dimensional weight is defined as $\boldsymbol{W}(R, u)$ whose element of the nth row and the kth column is

$$w_{n,k}(R, u) = e^{-jn\Theta(1+\xi)(u+u_0)} e^{-jk\Phi(R+R_0)} e^{jk(1+k\xi)\Psi v_0} \tag{14}$$

where $R \in [-\Delta R/2, \Delta R/2]$ and $u \in [-\Delta u/2, \Delta u/2]$.

Then the range-angle beamformer output is the 2-D HRRP of unresolved targets, expressed as

$$\begin{aligned} O(R, u) &= \text{vec}\,(\boldsymbol{W})^H \,\text{vec}\,(\boldsymbol{X}) \\ &= \sum_{m=1}^{M}\sum_{n=1}^{N}\sum_{k=1}^{K} A_m e^{-jn\Theta(1+k\xi)(\bar{u}_m-u)} \\ &\quad \cdot e^{-jk\Phi(\bar{R}_m-R)} e^{jk(1+k\xi)\Psi\bar{v}_m} \end{aligned} \tag{15}$$

where $\bar{R}_m = R_m - R_0$, $\bar{u}_m = u_m - u_0$, $\bar{v}_m = v_m - v_0$ and vec$(\cdot)$ denotes the vectorization operator.

High range resolution is determined by the synthetic bandwidth $B = K\Delta f$. To avoid the range ambiguity, Δf should not be larger than B_p [14]. We aim to separate the unresolved targets in range domain with 2-D HRRP. In this sense, the high range resolution is just close to target size and the synthetic bandwidth is still in the scope of narrowband. That is, $B \ll f_0$. In the sequel, (15) is approximated as (see Appendix B)

$$\begin{aligned} O(R, u) &\approx \sum_{m=1}^{M}\sum_{n=0}^{N-1}\sum_{k=0}^{K-1} A_m e^{-j[n\Theta(\bar{u}_m-u)+k\Phi(\bar{R}_m-R)-k\Psi\bar{v}_m]} \\ &= \sum_{m=1}^{M} A'_m \frac{\sin[N\Theta(u-\bar{u}_m)/2]}{\sin[\Theta(u-\bar{u}_m)/2]} \\ &\quad \cdot \frac{\sin[K\Phi(R-\bar{R}_m+\Psi/\Phi\bar{v}_m)/2]}{\sin[\Phi(R-\bar{R}_m+\Psi/\Phi\bar{v}_m)/2]} \end{aligned} \tag{16}$$

where $A'_m = A_m e^{-j\{\frac{N-1}{2}\Theta(\bar{u}_m-u)+\frac{K-1}{2}[\Phi(\bar{R}_m-R)-\Psi\bar{v}_m]\}}$. From (16), the range and angle resolutions of 2-D HRRP are

$$\begin{aligned} \Delta R' &= c/2B_pK \\ \Delta u' &= c/f_0Nd \end{aligned} \tag{17}$$

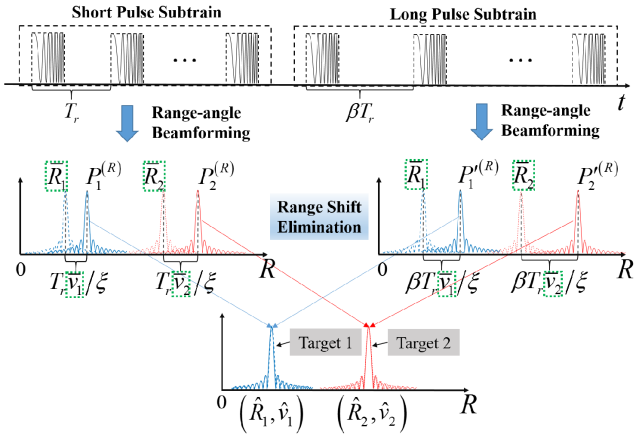

FIGURE 2. Illustration of short-long stepped-frequency pulse train for range shift elimination.

It is observed that the angle resolution of 2-D HRRP is unchanged but the range resolution turns to be $\Delta R/K$. In particular, the range resolution of 2-D HRRP $\Delta R'$ is corresponding to the stepped-frequency pulse train, which is different from the coarse range resolution of a single pulse ΔR. The diverse frequency in each pulse is synthesized to a large bandwidth which improves the range resolution ability. Then the coarse range resolution cell can be divided into K high range resolution cells. Thus, the unresolved targets can be separated only if the improved range resolution is less than targets' range difference. Different from the 1-D HRRP corresponding to each element, there is no coupling between range and angle in the 2-D HRRP. Target echo can be effectively integrated both in time and spatial domains. Thus, the 2-D HRRP we developed here is more suitable to the phased array radar. By generating the 2-D HRRP, the targets' angles can be determined directly.

However, the range-angle beamforming is not enough. From (16), the peaks of 2-D HRRP are located at

$$\begin{aligned}(P_m^{(R)}, P_m^{(u)}) &\approx (\bar{R}_m - \frac{\Psi}{\Phi}\bar{v}_m, \bar{u}_m) \\ &= (\bar{R}_m - \frac{T_r\bar{v}_m}{\xi}, \bar{u}_m) \end{aligned} \tag{18}$$

It should be noted that the peaks of 2-D HRRP still suffers from range shift caused by target motion. Such range shift will not only result in the inaccurate estimation of range and velocity, but also the missed detection when the shifted peaks are exactly overlapped.

B. PARAMETER ESTIMATION WITH RANGE SHIFT ELIMINATION

From (18), the angle can be determined directly but the range is still coupled with the velocity. Note that, the range shift caused by target motion is nearly linear to T_r. To solve two unknowns, we need two pulse trains with different PRI at least to determine the targets' velocities and eliminate the range shift.

Inspired by the methods of waveform design mentioned in Section I, a short-long stepped-frequency pulse train is specially designed as transmit waveform here. As shown in Fig. 2, the designed pulse train is combined with a short pulse subtrain with small PRI T_r and a long pulse subtrain with larger PRI βT_r. Two 2-D HRRPs with different range shift can be derived from the pulse subtrains by range-angle beamforming. Assume that the target peaks are fully detected (The detail of target detection is given in next subsection). The range shift can be eliminated by combining the target peaks of two 2-D HRRPs.

The peak postions of the first 2-D HRRP are given in (18). The peak postions of the second 2-D HRRP are

$$(P_m'^{(R)}, P_m'^{(u)}) \approx (\bar{R}_m - \beta\frac{T_r\bar{v}_m}{\xi}, \bar{u}_m) \tag{19}$$

By combining (18) and (19), two linear equations of targets' ranges and velocities are given as

$$\begin{cases} P_m^{(R)} = \bar{R}_m - \dfrac{T_r\bar{v}_m}{\xi} \\ P_m'^{(R)} = \bar{R}_m - \dfrac{\beta T_r\bar{v}_m}{\xi} \end{cases} \tag{20}$$

By solving (20), we can derive the estimations of range and angle as

$$\hat{R}_m = R_0 + \frac{\beta P_m^{(R)} - P_m'^{(R)}}{\beta - 1} \tag{21a}$$

$$\hat{v}_m = v_0 + \frac{\xi\left(P_m^{(R)} - P_m'^{(R)}\right)}{(\beta-1)\,T_r} \tag{21b}$$

As mentioned above, the beamformer outputs of short pulse subtrain and long pulse subtrain both can determine target angle directly. To improve the estimation performance, the average value is used as the angle estimation. Then we have

$$\hat{u}_m = \frac{P_m^{(u)} + P_m'^{(u)}}{2} \tag{22}$$

C. BEAMFORMING DETECTION

An key assumption of accurate parameters estimation is that all target peaks of 2-D HRRP are detected successfully. In general, missed detection and false alarm are inevitable in the process of target detection. However, the false alarm is more acceptable than the missed detection because the false target will not affect the parameters estimation of real targets. Moreover, the false alarm probability can be kept around a constant by the CFAR technique.

The Cell Averaging (CA) CFAR and the Ordered Statistic (OS) CFAR are commonly used in the two-dimensional target detection. However, it is known that the CA CFAR procedure has a main drawback and leads to some masking effects in multitarget situations. The OS CFAR is proposed to avoid the described masking effects [25]. Therefore, we use the OS CFAR here to detect the unresolved targets. Note that, a range-Doppler matrix derived by matching filtering and MTD processing is usually used in the conventional target detection. Here, it is replaced by the 2-D HRRP which is a range-angle matrix.

TABLE 1. Parameters of radar.

Parameter	Value	Parameter	Value
Element number N	16	Pulse number K	10
Pulse duration T_p	75μs	PRI T_r	1ms
Carrier frequency f_0	1GHz	Frequency increment Δf	1MHz
LFM bandwidth B_p	1MHz	Element interval d	0.15m

Assume that the 2-D HRRP contains $P \times Q$ data cells. To determine the detection threshold, we use $P_{\mathrm{R}} \times Q_{\mathrm{R}}$ reference window to estimate the interference statistic. A $P_{\mathrm{G}} \times Q_{\mathrm{G}}$ guard window is usually introduced surrounding the test cell because the cells in guard window may contain target returns, which will bias the interference estimate. Thus, the number of available cells in reference window is $N_{\mathrm{R}} = P_{\mathrm{R}} \times Q_{\mathrm{R}} - P_{\mathrm{G}} \times Q_{\mathrm{G}}$. In the OS CFAR procedure, the data cells $\{O_1, O_2, \cdots, O_{N_{\mathrm{R}}}\}$ contained in reference window is sorted according to their magnitude as $\{O_{(1)}, O_{(2)}, \cdots, O_{(N_{\mathrm{R}})}\}$ where

$$O_{(1)} < O_{(2)} < \cdots < O_{(i)} < \cdots < O_{(N_{\mathrm{R}})} \tag{23}$$

The ith value is selected to indicate the average interference floor and the decision threshold is

$$T = \gamma_{\mathrm{OS}} O_{(\mathrm{i})} \tag{24}$$

where γ_{OS} is the threshold factor. The probability of false alarm P_{fa} is expressed [26]

$$P_{\mathrm{fa}} = \frac{N_{\mathrm{R}}!(\gamma_{\mathrm{OS}} + N_{\mathrm{R}} - i)!}{(N_{\mathrm{R}} - i)!(\gamma_{\mathrm{OS}} + N_{\mathrm{R}})!} \tag{25}$$

To maintain the false alarm P_{fa}, the threshold factor γ_{OS} needs to be determined according to (25). A reasonable value of $i = 0.75N_{\mathrm{R}}$ is usually used to achieve a CFAR loss near the minimum [27]. Note that, the actual probability of false alarm may be a little higher than the theoretical value in (25) especially at low SNR, since the overlapped sidelobe peak of multiple targets may be detected.

IV. SIMULATION RESULTS

In this section, we consider the scenario where a linear array radar transmits stepped-frequency LFM pulse train to detect and measure the unresolved targets. The radar parameters are given in Table 1. In this radar system, the coarse range resolution, angle resolution and velocity resolution are $\Delta R = 150$m, $\Delta u = 0.125$ and $\Delta v = 15$m/s respectively. The range resolution can be improved to 15m by synthesizing the diverse bandwidth of each pulse. Meanwhile, the whole coarse resolution cell can be divided into 10 high range resolution cells. Fig. 3 shows three cases of unresolved targets and each target's parameters. All targets are located in the same coarse resolution cell (60km, 0.1, 100m/s) and we assume targets' SNRs are all equal to 10dB. There are three targets in Case 1 and Case 3, but two targets in Case 2 where the middle target is deleted. In addition, Target 2 and Target 3 of Case 3 are much closely-spaced in range and velocity. Their range difference is less than a high range resolution cell.

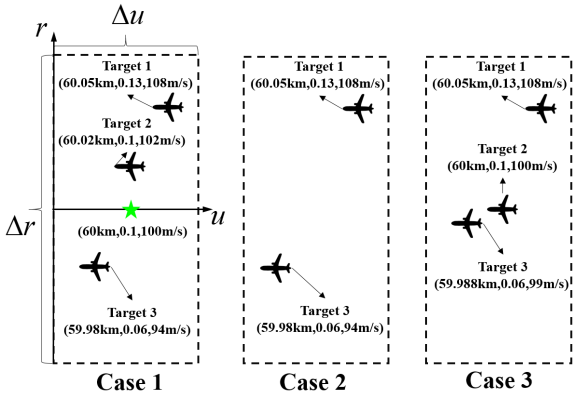

FIGURE 3. Three cases of unresolved targets.

First, we consider the conventional stepped-frequency LFM pulse train. The 2-D HRRPs in three cases derived by range-angle beamforming are shown in Fig. 4. As to three cases of unresolved targets, it is easy to distinguish the peak corresponding to each target. Note that, the resolution performance can be improved by combining multiple domains. Thus, Target 2 and Target 3 in Case 3 are still resolved in range-angle domain even though their range difference is less than a high range resolution cell. However, the peak position deviates from the true target's position both in range and angle domains. The shift in range domain is caused by the target motion and the shift in angle domain is caused by the approximation of model. It is observed that the sidelobe keeps around -11dB in Case 1 and Case 2, but rises to -8.5dB in Case 3. That is, the sidelobe will increase when two targets get closed, which results in the deterioration of detection performance. We may suppress the sidelobe by adding the windowing. But such processing will reduce the resolution both in range and angle domains.

Next, we focus on another stepped-frequency LFM pulse train whose PRI is βT_r. Fig. 5 shows each target's range shift versus PRI of three cases. It is observed that the range shift of each target is nearly linear to the PRI of transmitted pulse train, which is coincident with the analysis given in (18). That is, the designed short-long stepped-frequency pulse train is feasible to eliminate the range shift. However, the range shifts corresponding to Target 2 and Target 3 in Case 3 deviates from the true values, which may result in a severe estimation errors of target's range and velocity. Thus, the approximation presented in (18) will be biased if two targets are mcuh closely-spaced. In addition, the approximate value of range shift fluctuates around the true value. The approximate error is related to target parameters. It is much difficult to correct such error because the target parameters are unknown before transmitting. Therefore, the optimal value of β involved in the proposed short-long stepped-frequency pulse train cannot be explored in theory.

Then, we use the designed short-long stepped-frequency pulses train to estimate the parameters of unresolved targets where β is set as 1.5, 1.75 and 2. The method proposed in [17] is chosen as the baseline method for comparison, where the

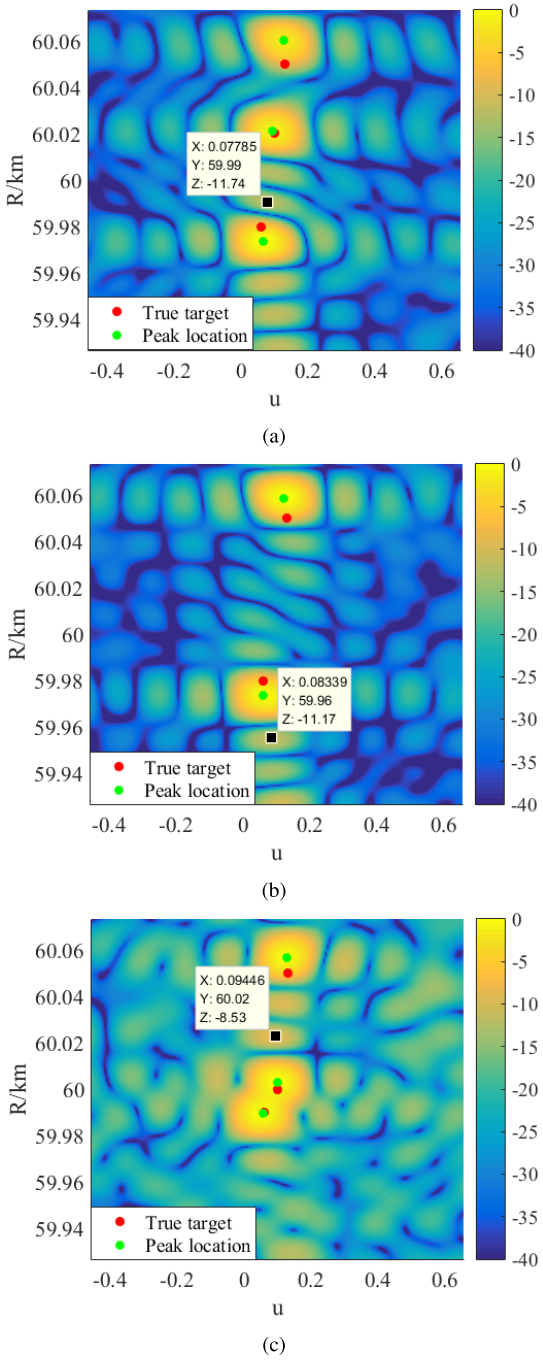

FIGURE 4. 2-D HRRPs of unresolved targets of (a) Case 1, (b) Case 2 and (c) Case 3.

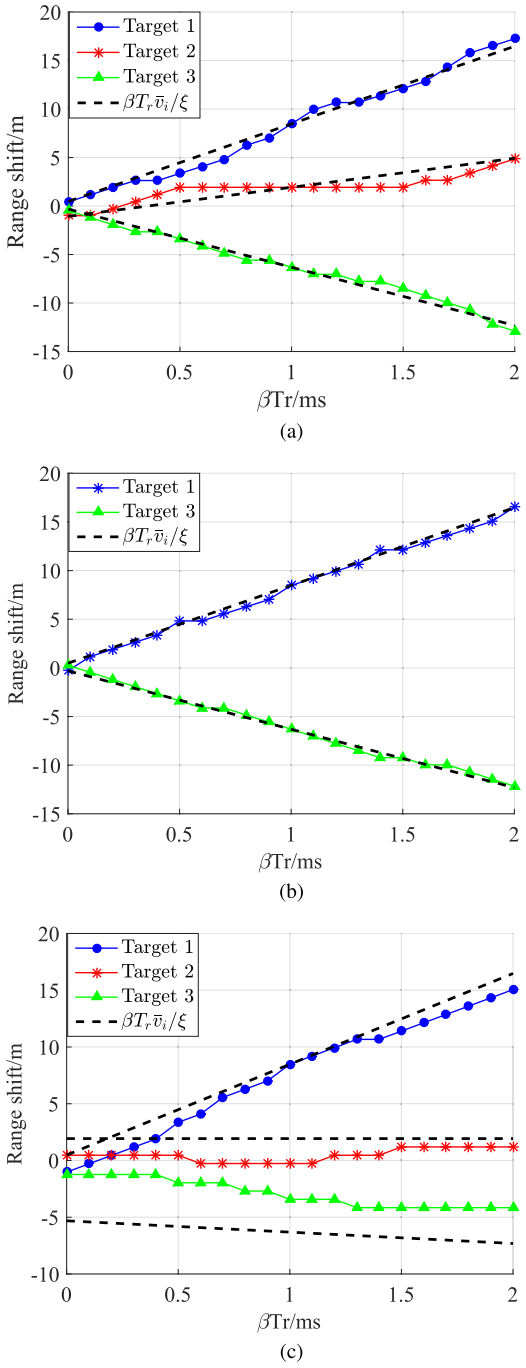

FIGURE 5. Range shift of each target versus PRI in (a) Case 1, (b) Case 2, and (c) Case 3.

target number is estimated by MDL principle and the target's parameters are estimated by ML principle. To assess the estimation performance, 100 trials are run to calculate the Root Mean Square Error (RMSE). Here, the RMSE is the average estimation error of all targets. Fig. 6 shows the RMSEs of range, angle and velocity in three cases. It is observed that the range shift is eliminated by the designed waveform and the estimated result is unbiased. Note that, the proposed method outperforms ML estimation at low SNR. A high SNR is required for the ML estimation to achieve a good performance because not only target's parameters need to be estimated, but also its echo amplitude. In contrary, the effective range-angle integration of the proposed method provides a high beamforming peak of target for the accurate parameter estimation. It should be noted that the estimation errors of Case 3 are much larger than other two cases. However, the closely-spaced targets have little influence on the performance of ML estimation, which is its distinct advantage. In addition, it is found that the estimation errors in range and velocity are the smallest when β is equal to 2. That is, a better estimation

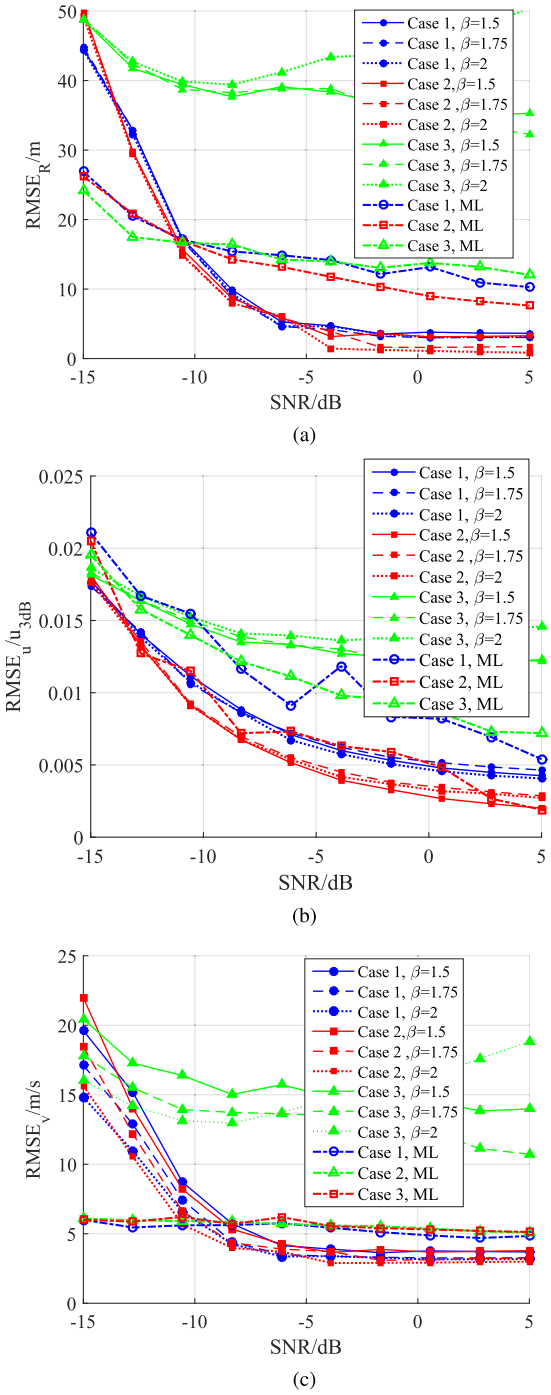

FIGURE 6. RMSE of parameter estimation in three cases: (a) range, (b) angle and (c) velocity.

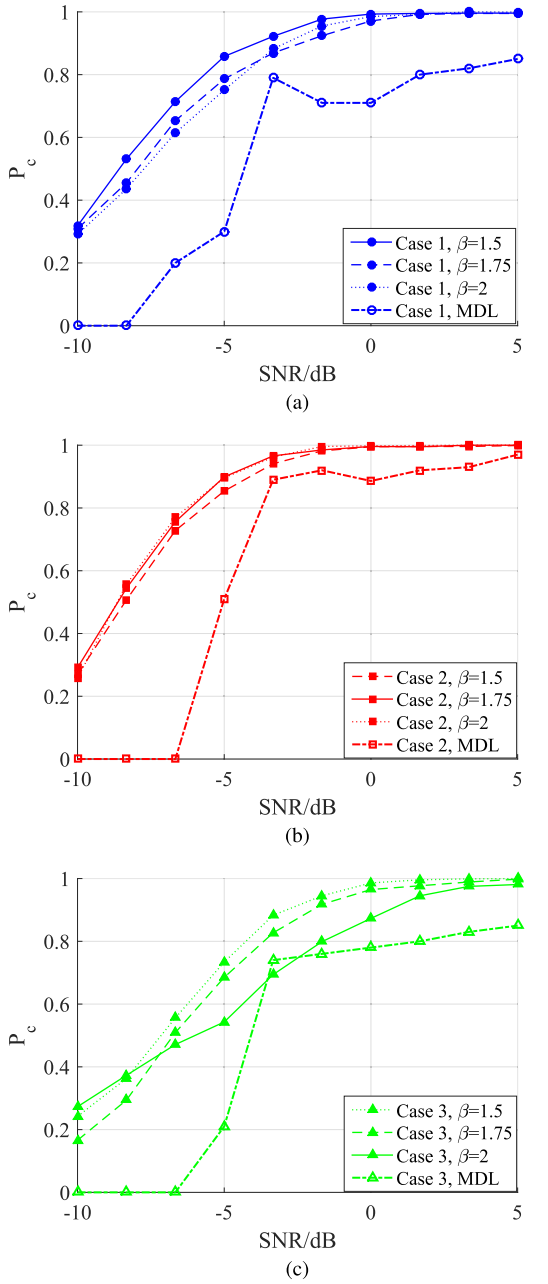

FIGURE 7. Correct detection probability of three cases versus SNR: (a) Case 1, (b) Case 2 and (c) Case 3.

performance can be achieved by using a longer pulse subtrain since the range and velocity estimations are inverse proportional to β as shown in (21a) and (21b). However, a longer observation time is required when choosing a large β, which may be limited in the real application. Therefore, a trade-off should be made between the estimation performance and the observation time.

The detection performance of unresolved targets is also tested. 100 trials are also run to calculate the correct probability of detection P_c where β is set as 1.5, 1.75 and 2. Note that, there are two 2-D HRRPs derived from the designed short-long frequency pulse train. A successful detection is counted when all targets are detected both in two 2-D HRRPs. Regarding the target detection by MDL, we set the maximum value of target number as 4 for an acceptable computationa cost. Fig. 7 shows the correct detection probability of three cases versus SNR. It is observed that the unresolved targets in three cases can be successfully detected even at low SNR since the target echo is effectively integrated in time and spatial domains. Obviously, the proposed method outperfoms MDL detection because MDL detection requires a high SNR especially in the case of unresolved targets.

TABLE 2. Average computational time.

	Case 1	Case 2	Case 3
The proposed method	1.01s	0.94s	0.94s
MDL + ML	143.36s	64.98s	125.79s

The detection performance of Case 2 is the best and the detection performance of Case 3 is the worst. That is, the detection performance has a deterioration when handling more targets or closely-spaced targets. Moreover, the detection performance of Case 3 has a improvement with β increasing. This is mainly because that a long pulse subtrain results in a large range shift which is beneficial to the detection for closely-spaced targets.

Finally, we give the average computational times of the proposed method and the baseline method in Table 2. The algorithms are programmed in Matlab 2015 and run in the platform with a 2.5-GHz Intel i5-7200U CPU. It is observed that the computational time of the proposed method is much lower than that of the baseline method. Moreover, it still keeps around a low value even for more targets. The proposed method can detect and measure the unresolved targets in real time. In contrary, the combination of MDL and ML requires a high computational cost which limits its application in practice use. Thus, the proposed method outperforms the baseline method in computational cost.

V. CONCLUSION

In this paper, a novel scheme to detect and measure the unresolved targets is proposed for the phased array radar by transmitting stepped-frequency waveform. We design a short-long stepped-frequency pulse train and use the range-angle beamforming technique to derive two 2-D HRRPs. By combining two 2-D HRRPs, each target can be detected successfully and targets' parameters can be estimated accurately. Some conclusions are drawn from the simulation results as following. 1. The pulse train with large PRI is beneficial to improve the performance of parameter estimation, but more observation time is required. A trade-off between estimation performance and observation time in the waveform design is needed. 2. The performance of detection and parameter estimation will get worse when targets are much closely-spaced in range and velocity.

APPENDIX A
MATCHING FILTER OUTPUT OF STEPPED-FREQUENCY LFM PULSE TRAIN

Inserting (1) into (3), the matching filter output is rewritten as

$$\begin{aligned} Z_n(t) &= \alpha e^{-j\frac{2\pi}{c}f_k ndu}\sum_{k=0}^{K-1}\int_{-\infty}^{\infty} p\left(\tau-\frac{2R}{c}+\frac{2v\tau}{c}-kT_r\right) \\ &\quad\cdot p^*(\tau-t)e^{2\pi f_k(\tau-\frac{2R}{c}+\frac{2v\tau}{c})}e^{j2\pi f_k(\tau-t)}\mathrm{d}\tau \\ &\overset{\text{def}}{=} \alpha e^{-j\frac{2\pi}{c}f_k ndu}\sum_{k=0}^{K-1} z_k(t) \end{aligned} \tag{26}$$

where $z_k(t)$ denotes the filter output of each pulse. Let $s=\tau-\frac{2R}{c}+\frac{2v\tau}{c}-kT_r$, $z_k(t)$ is expressed as

$$\begin{aligned} z_k(t) &= e^{j2\pi f_k t}e^{-j2\pi f_k\frac{2R}{c+2v}}e^{j2\pi f_k\frac{2kT_r v}{c+2v}} \\ &\quad\cdot\int_{-\infty}^{\infty} p(s)\,p^*\left[\frac{c}{c+2v}\left(s+\frac{2R}{c}+kT_r\right)-t\right]e^{j2\pi f_k\frac{2v}{c+2v}s}\mathrm{d}s \end{aligned} \tag{27}$$

In general, target's velocity is more less than the light speed, that is $v \ll c$. Then $z_k(t)$ can be approximately expressed as

$$\begin{aligned} z_k(t) &\approx e^{j2\pi f_k t}e^{-j2\pi f_k\frac{2R}{c}}e^{j2\pi f_k\frac{2kT_r v}{c}} \\ &\quad\cdot\int_{-\infty}^{\infty} p(s)\,p^*\left[s-\left(t-\frac{2R}{c}-kT_r\right)\right]e^{j2\pi f_k\frac{2v}{c}s}\mathrm{d}s \\ &= \chi\left(t-\frac{2R}{c}-kT_r, f_k\frac{2v}{c}\right)e^{j2\pi f_k t}e^{-j4\pi f_k\frac{R-kT_r v}{c}} \end{aligned} \tag{28}$$

where $\chi(t,f_d) = \int_{-\infty}^{\infty} p(\tau)p^*(\tau-t)e^{j2\pi f_d}\mathrm{d}\tau$. Indeed, $|\chi(t,f_d)|$ is the ambiguity function of LFM waveform and $\chi(t,f_d)$ is expressed as

$$\chi(t,f_d)=\left|\frac{\sin[\pi(f_d+\mu t)(T_p-|t|)]}{T_p\pi(f_d+\mu t)}\right|e^{j\pi[(f_d-\mu t)(T_p-t)-\mu t^2]} \tag{29}$$

Here, we define $\phi(t)$ as the phase of $\chi(t-2R/c-kT_r, f_k 2v/c)$. In the sequel, (26) is rewritten as

$$\begin{aligned} Z_n(t) &= \alpha\sum_{k=0}^{K-1}\left|\chi\left(t-\frac{2R}{c}-kT_r, \frac{2v}{c}f_k\right)\right| \\ &\quad\times e^{-j\frac{4\pi}{c}f_k(R+\frac{ndu}{2}-kT_r v)}e^{-j2\pi f_k t+\phi(t)} \end{aligned} \tag{30}$$

We use $e^{-j2\pi f_k t}$ as the reference signal to demodulate the filtered signal. After such demodulation processing, the baseband signal is derived as

$$Z_n'(t) = \alpha'\sum_{k=0}^{K-1}\left|\chi\left(t-\frac{2R}{c}-kT_r, \frac{2v}{c}f_k\right)\right|e^{-j\frac{4\pi}{c}f_k(R+\frac{ndu}{2}-kT_r v)} \tag{31}$$

where $\alpha'=\alpha e^{-j\frac{4\pi}{c}f_0 R+\phi(t)}$. The exponential term in (31) can be rewritten as

$$\begin{aligned} &e^{-j\frac{4\pi}{c}f_k(R+\frac{ndu}{2}-kT_r v)} \\ &= e^{-j\frac{4\pi}{c}f_0 R}e^{-j\frac{2\pi}{c}f_0 ndu}e^{-j\frac{2\pi}{c}k(2\Delta fR-2f_0T_r v+\Delta fndu)} \\ &\quad\cdot e^{j\frac{4\pi}{c}k^2\Delta fT_r v} \\ &\overset{\text{def}}{=} e^{-j\frac{4\pi}{c}f_0 R}e^{-jn\Theta u}e^{-jk(\Phi R-\Psi v+n\xi\Theta u)}e^{jk^2\xi\Psi v} \end{aligned} \tag{32}$$

where $\Theta = 2\pi f_0 d/c$ $\Phi = 4\pi\Delta f/c$, $\Psi = 4\pi T_r f_0/c$, and $\xi = f_0/\Delta f$. Inserting (32) into (31), $Z_n'(t)$ is rewritten as

$$\begin{aligned} Z_n'(t) &= \alpha'\sum_{k=0}^{K-1}\left|\chi\left(t-\frac{2R}{c}-kT_r, \frac{2v}{c}f_k\right)\right| \\ &\quad\cdot e^{-jn\Theta u}e^{-jk(\Phi R-\Psi v+n\xi\Theta u)}e^{jk^2\xi\Psi v} \end{aligned} \tag{33}$$

APPENDIX B
APPROXIMATION OF (14)

It is observed from (15) that there are three phase terms related to target range, angle and velocity respectively. However, it is difficult to derive the closed-form formulation due to cross phase terms $\varphi_m^{(u)} = -kn\xi\Theta(u-\bar{u}_m)$ and quadratic phase term $\varphi_m^{(v)} = k^2\xi\Phi\bar{v}_m$.

Since the variation section of R_m, u_m and v_m are all in one resolution cell, we define $\bar{R}_m = R_m - R_0 = a_m R_{3\text{dB}}$, $\bar{u}_m = u_m - u_0 = b_m u_{3\text{dB}}$ and $\bar{v}_m = v_m - v_0 = c_m v_{3\text{dB}}$, where a_m, b_m and c_m are the constants between -0.5 and 0.5. Then we have

$$\begin{aligned}\left|\varphi_m^{(u)}\right| &= |kn\xi\Theta(u-b_m\Delta u)| \le kn\xi\Theta\Delta u \\ &= kn\frac{\Delta f}{f_0}\frac{2\pi f_0 d}{c}\frac{c}{f_0 N d} \\ &= 2\pi\frac{n}{N}\frac{k\Delta f}{f_0} \le 2\pi\frac{B}{f_0} \end{aligned} \tag{34}$$

$$\begin{aligned}\left|\varphi_m^{(v)}\right| &= \left|k^2\xi\Phi b_m\Delta v\right| \le k^2\xi\Phi\Delta v \\ &= \pi b_m k^2\frac{\Delta f}{f_0}\frac{4\pi f_0 T_r}{c}\frac{c}{2f_0 K T_r} \\ &= 2\pi b_m\frac{n}{N}\frac{k\Delta f}{f_0} \le 2\pi\frac{B}{f_0} \end{aligned} \tag{35}$$

As mentioned above, the synthetic bandwidth is much less the carrier frequency which is $B \ll f_0$. Thus, the phase terms $\varphi_m^{(u)}$ and $\varphi_m^{(v)}$ can be ignored. Then (15) is rewritten as

$$\begin{aligned} O(R,u) &\approx \sum_{m=1}^{M}\sum_{n=0}^{N-1}\sum_{k=0}^{K-1} A_m e^{-j[n\Theta(\bar{u}_m-u)+k\Phi(\bar{R}_m-R)-k\Psi\bar{v}_m]} \\ &= \sum_{m=1}^{M} A'_m\frac{\sin[N\Theta(u-\bar{u}_m)/2]}{\sin[\Theta(u-\bar{u}_m)/2]} \\ &\quad\cdot\frac{\sin[K\Phi(R-\bar{R}_m+\Psi/\Phi\bar{v}_m)/2]}{\sin[\Phi(R-\bar{R}_m+\Psi/\Phi\bar{v}_m)/2]} \end{aligned} \tag{36}$$

where $A'_m = A_m e^{-j\{\frac{N-1}{2}\Theta(\bar{u}_m-u)+\frac{K-1}{2}[\Phi(\bar{R}_m-R)-\Psi\bar{v}_m]\}}$.

REFERENCES

[1] W. D. Blair and M. Brandt-Pearce, "Unresolved Rayleigh target detection using monopulse measurements," *IEEE Trans. Aerosp. Electron. Syst.*, vol. 34, no. 2, pp. 543–552, Apr. 1998.

[2] K. S. Kulpa and Z. Czekala, "Masking effect and its removal in PCL radar," *IEE Proc.-Radar, Sonar Navigat.*, vol. 152, no. 3, pp. 174–178, Jun. 2005.

[3] W. D. Blair and M. Brandt-Pearce, "Statistical description of monopulse parameters for tracking Rayleigh targets," *IEEE Trans. Aerosp. Electron. Syst.*, vol. 34, no. 2, pp. 597–611, Apr. 1998.

[4] W. D. Blair and M. Brandt-Pearce, "Monopulse DOA estimation of two unresolved Rayleigh targets," *IEEE Trans. Aerosp. Electron. Syst.*, vol. 37, no. 2, pp. 452–469, Apr. 2001.

[5] A. Sinha, T. Kirubarajan, and Y. Bar-Shalom, "Maximum likelihood angle extractor for two closely spaced targets," *IEEE Trans. Aerosp. Electron. Syst.*, vol. 38, no. 1, pp. 183–203, Jan. 2002.

[6] Z. Wang, A. Sinha, P. Willett, and Y. Bar-Shalom, "Angle estimation for two unresolved targets with monopulse radar," *IEEE Trans. Aerosp. Electron. Syst.*, vol. 40, no. 3, pp. 998–1019, Jul. 2004.

[7] N. Nandakumaran, A. Sinha, and T. Kirubarajan, "Joint detection and tracking of unresolved targets with monopulse radar," *IEEE Trans. Aerosp. Electron. Syst.*, vol. 44, no. 4, pp. 1326–1341, Oct. 2008.

[8] Y. Zheng, S.-M. Tseng, and K.-B. Yu, "Closed-form four-channel monopulse two-target resolution," *IEEE Trans. Aerosp. Electron. Syst.*, vol. 39, no. 3, pp. 1083–1089, Jul. 2003.

[9] D. F. Crouse, U. Nickel, and P. Willett, "Comments on 'Closed-form four-channel monopulse two-target resolution,'" *IEEE Trans. Aerosp. Electron. Syst.*, vol. 48, no. 1, pp. 913–916, Jan. 2012.

[10] X. Zhang, P. K. Willett, and Y. Bar-Shalom, "Monopulse radar detection and localization of multiple unresolved targets via joint bin processing," *IEEE Trans. Signal Process.*, vol. 53, no. 4, pp. 1225–1236, Apr. 2005.

[11] J. D. Glass and W. D. Blair, "Detection of Rayleigh targets using adjacent matched filter samples," *IEEE Trans. Aerosp. Electron. Syst.*, vol. 51, no. 3, pp. 1927–1941, Jul. 2015.

[12] J. D. Glass, W. D. Blair, and A. D. Lanterman, "Joint-bin monopulse processing of Rayleigh targets," *IEEE Trans. Signal Process.*, vol. 63, no. 24, pp. 6673–6683, Dec. 2015.

[13] S. He, W. Zhang, and G. Guo, "High range resolution MMW radar target recognition approaches with application," in *Proc. IEEE Nat. Aerosp. Electron. Conf. (NAECON)*, vol. 1, May 1996, pp. 192–195.

[14] T. Long and L. Ren, "HPRF pulse Doppler stepped frequency radar," *Sci. China F, Inf. Sci.*, vol. 52, no. 5, pp. 883–893, May 2009.

[15] Y. Liu, H. Meng, G. Li, and X. Wang, "Range-velocity estimation of multiple targets in randomised stepped-frequency radar," *Electron. Lett.*, vol. 44, no. 17, pp. 1032–1034, Aug. 2008.

[16] Y. Liu, H. Meng, G. Li, and X. Wang, "Velocity estimation and range shift compensation for high range resolution profiling in stepped-frequency radar," *IEEE Geosci. Remote Sens. Lett.*, vol. 7, no. 4, pp. 791–795, Oct. 2010.

[17] Y. Liu, H. Meng, H. Zhang, and X. Wang, "Motion compensation of moving targets for high range resolution stepped-frequency radar," *Sensors*, vol. 8, no. 5, pp. 3429–3437, May 2008.

[18] G. Li, H. Meng, X.-G. Xia, and Y.-N. Peng, "Range and velocity estimation of moving targets using multiple stepped-frequency pulse trains," *Sensors*, vol. 8, no. 2, pp. 1343–1350, 2008.

[19] H.-Y. Chen, Y.-X. Liu, W.-D. Jiang, and G.-R. Guo, "A new approach for synthesizing the range profile of moving targets via stepped-frequency waveforms," *IEEE Geosci. Remote Sens. Lett.*, vol. 3, no. 3, pp. 406–409, Jul. 2006.

[20] Z. Yong-Feng, Z. Hong-Zhong, and F. Qiang, "Simultaneously velocity measuring and HRR profiling with a novel CSF sequence," in *Proc. CIE Int. Conf. Radar*, Oct. 2006, pp. 1–5.

[21] M. A. Temple, K. L. Sitler, R. A. Raines, and J. A. Hughes, "High range resolution (HRR) improvement using synthetic HRR processing and stepped-frequency polyphase coding," *IEE Proc.-Radar, Sonar Navigation*, vol. 151, no. 1, pp. 41–47, Feb. 2004.

[22] M. Y. Chua, V. C. Koo, H. S. Lim, and J. T. S. Sumantyo, "Phase-coded stepped frequency linear frequency modulated waveform synthesis technique for low altitude ultra-wideband synthetic aperture radar," *IEEE Access*, vol. 5, pp. 11391–11403, 2017.

[23] P.-P. Pan, H. Liu, Y.-X. Zhang, W. Qi, and Z.-M. Deng, "Range, radial velocity, and acceleration MLE using frequency modulation coded LFM pulse train," *Digit. Signal Process.*, vol. 60, pp. 252–261, Jan. 2017.

[24] S. L. Wang, Z.-H. Xu, X. Liu, W. Dong, and G. Wang, "Subarray-based frequency diverse array for target range-angle localization with monopulse processing," *IEEE Sensors J.*, vol. 18, no. 14, pp. 5937–5947, Jul. 2018.

[25] M. Kronauge and H. Rohling, "Fast two-dimensional CFAR procedure," *IEEE Trans. Aerosp. Electron. Syst.*, vol. 49, no. 3, pp. 1817–1823, Jul. 2013.

[26] H. Rohling, "Radar CFAR thresholding in clutter and multiple target situations," *IEEE Trans. Aerosp. Electron. Syst.*, vol. AES-19, no. 4, pp. 608–621, Jul. 1983.

[27] M. Richards, J. Scheer, and W. Holm, *Principles of Modern Radar: Basic Principles*. Rijeka, Croatia: SciTech, 2010.

SHENGBIN LUO WANG was born in Jiangxi, China. He received the B.S. degree in information and communication engineering from the National University of Defense Technology (NUDT), Changsha, China, in 2017, where he is currently pursuing the Ph.D. degree with the State Key Laboratory of Complex Electromagnetic Environment Effects.

His research interests include frequency diverse array, phased array signal processing, and radar signal processing.

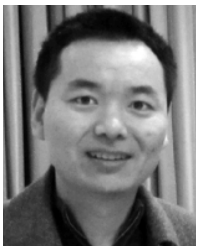

ZHEN-HAI XU was born in 1977. He received the B.E. and Ph.D. degrees in electronic engineering from the National University of Defense Technology (NUDT), Hunan, China, in 1998 and 2004, respectively, where he is currently a Professor.

He was with the Nanjing Research Institute on Electronic Technology, from 2006 to 2008. His research interests include array signal processing and radar polarimetry.

XINGHUA LIU was born in Gansu, China. He received the B.S. degree in electronic engineering from the National University of Defense Technology (NUDT), Changsha, China, in 2015, where he is currently pursuing the Ph.D. degree with the State Key Laboratory of Complex Electromagnetic Environment Effects.

His research interests include MIMO radar, distributed radar, and radar signal processing.

WEI DONG was born in Jiangxi, China. He received the B.S. degree in electronic engineering from the National University of Defense Technology (NUDT), Changsha, China, in 2017, where he is currently pursuing the Ph.D. degree with the State Key Laboratory of Complex Electromagnetic Environment Effects.

His research interests include subarray partition and compressed sensing.

GUOYU WANG received the Ph.D. degree in information and communication engineering from the National University of Defense Technology (NUDT), Changsha, China, in 1999, where he is currently a Professor.

His research interests include signal processing, radar system simulation, and electromagnetic environment effects.